

# SmartCon: Deep Probabilistic Learning Based Intelligent Link-Configuration in Narrowband-IoT Towards 5G and B5G

Raja Karmakar, *Member, IEEE*, Georges Kaddoum, *Senior Member, IEEE*  
and Samiran Chattopadhyay, *Senior Member, IEEE*

**Abstract**—To enhance the coverage and transmission reliability, repetitions adopted by Narrowband Internet of Things (NB-IoT) allow repeating transmissions several times. However, this results in a waste of radio resources when the signal strength is high. In addition, in low signal quality, the selection of a higher modulation and coding scheme (MCS) level leads to a huge packet loss in the network. Moreover, the number of physical resource blocks (PRBs) per-user needs to be chosen dynamically, such that the utilization of radio resources can be improved on per-user basis. Therefore, in NB-IoT systems, dynamic adaptation of repetitions, MCS, and radio resources, known as *auto link-configuration*, is crucial. Accordingly, in this paper, we propose *SmartCon* which is a *Generative Adversarial Network (GAN)*-based deep learning approach for auto link-configuration during uplink or downlink scheduling, such that the packet loss rate is significantly reduced in NB-IoT networks. For the training purpose of the GAN, we use a *Multi-Armed Bandit (MAB)*-based reinforcement learning mechanism that intelligently tunes its output depending on the present network condition. The performance of *SmartCon* is thoroughly evaluated through simulations where it is shown to significantly improve the performance of NB-IoT systems compared to baseline schemes.

**Index Terms**—NB-IoT; link-configuration; modulation and coding scheme; repetitions; physical resource block

## I. INTRODUCTION

The number of Internet of Things (IoT) [1] devices is constantly increasing in the fifth-generation (5G) and beyond 5G (B5G) of mobile telecommunications. To meet the demands described by the IoT specifications, the Third Generation Partnership Project (3GPP) has presented a new radio access technology, known as Narrowband Internet of Things (NB-IoT) [2], [3]. NB-IoT can provide an improved coverage compared to Long-Term Evolution (LTE) networks, massive device connectivity, ultra-low device complexity or costs, and low power consumption [4]. Specifically, NB-IoT is a variant of LTE, designed for IoT frameworks. Like LTE, the NB-IoT technology is based on orthogonal frequency-division multiple access (OFDMA), with a system bandwidth of 180 kHz which is equal to one *physical resource block (PRB)* in 4G LTE transmissions. Given this low channel bandwidth, NB-IoT

R. Karmakar and G. Kaddoum are with Department of Electrical Engineering, ETS, University of Quebec, Montreal, Canada (Email: raja.karmakar.1@ens.etsmtl.ca, georges.kaddoum@etsmtl.ca).

S. Chattopadhyay is with Department of Information Technology, Jadavpur University, Kolkata, India 700098, and Institute for Advancing Intelligence, TCG Centres for Research and Education in Science and Technology, Kolkata, India (Email: samiran.chattopadhyay@jadavpuruniversity.in).

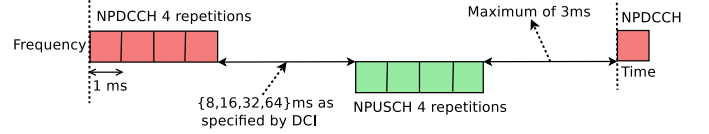


Fig. 1. An illustration of repetition

specifically focuses on indoor coverage, and data transmission with a higher latency [2], [3]. Dynamic adjustment to different radio conditions can be performed by configuring the *modulation and coding scheme (MCS)* value, which is defined as the combination of a type of modulation and coding rate used for a given PRB [5], [6]. The MCS is a key feature which is used to set the data rate of a transmission in a wireless connection [6]. In NB-IoT, the MCS value is between 0 and 12, with a variable Transport Block Size (TBS) [5], [7]. The MCS also specifies how many bits can be transferred per *resource element (RE)* which is the smallest modulation structure in LTE [3].

In order to achieve coverage enhancement and improve transmit reliability in NB-IoT, the concept of *repetitions* is used in the data and control signal transmissions [8], [9]. Repetitions imply repeating the transmission several times [6]. The repetition for the uplink and downlink transmissions can be selected from  $\{1, 2, 4, 8, 16, 32, 64, 128\}$  and  $\{1, 2, 4, 8, 16, 32, 64, 128, 256, 512, 1024, 2048\}$ , respectively, where the selected number denotes the number of repetition of the same transmission block [6]. Fig. 1 illustrates a repetition of 4 in NB-IoT with both Narrowband Physical Uplink Shared Channel (NPUSCH) and Narrowband Physical Downlink Control Channel (NPDCCH) transmission blocks, where the content of each of these blocks is repeated 4 times during a single transmission. The time gap between the NPDCCH and NPUSCH repetitions is defined by the downlink control information (DCI). It specifies a scheduling index that permits a device to collect data during downlink scheduling [10].

Since the transmission reliability is enhanced by the use of repetitions, it should be enabled when the signal strength is poor [11]. On the other hand, the MCS level needs to be chosen dynamically based on the signal strength [12]. When the channel conditions are poor, the selection of a high MCS value results in a higher *packet loss rate (PLR)*, and consequently the system throughput is reduced. Moreover, the rapid changes in channel conditions lead to high fluctuations in the PLR in NB-IoT networks [12], [13]. Therefore, during

scheduling, both MCS and repetitions play a crucial role in the packet transmission such that the best suited data rate, coverage and a low PLR can be achieved based on the present channel condition. Moreover, NB-IoT systems use radio resource blocks reserved by LTE systems [14], and thus appropriate utilization of radio resources is especially demanded for NB-IoT. Therefore, an adaptive selection of the number of PRBs per-user is also required in NB-IoT.

Therefore, during uplink or downlink scheduling, a dynamic adaptation, known as *auto link-configuration*, is required for MCS levels, repetitions, and per-user PRB in NB-IoT systems. Therefore, we can represent the auto link-configuration in NB-IoT as a three dimensional problem – (i) selection of MCS values, (ii) determination of the repetitions, and (iii) selection of the number of PRBs per-user.

### A. State-of-the-Art

An effective approach for small data transmission in NB-IoT is proposed in [15], without the consideration of the connection setup process related to radio resource control. However, this work does not focus on the adaptation of MCS and repetition number. Authors in [16] model the random access traffic in NB-IoT by considering the arrival of processes and their services, where the network delay is analyzed based on random latency bounds. The work [17] discusses the primary challenges of providing a stable connectivity to a huge number of machine-type communication (MTC) devices in NB-IoT networks. In [18], the proposed uplink scheduler for NB-IoT frameworks is a basic threshold-based approach with user equipment (UE) specific requirements, which is mainly suitable for homogeneous traffic. Details and the uplink and downlink transmission channels' performance are discussed in [19] with a focus on the design approaches in NB-IoT. Yu *et al.* [12] propose an uplink scheduling mechanism for NB-IoT, where the uplink link adaptation, including the determination of the MCS value and repetition number, is performed based on the present channel condition. However, this work does not consider downlink scheduling and it uses a threshold-based mechanism for the MCS and repetitions selection in NB-IoT systems.

In the direction of resource management, the work [14] designs a mechanism for resource allocation in NB-IoT, by focusing only on the rate maximization. Manne *et al.* [20] explain NPDCCH physical layer procedures with the technique of search space decoding, where a resource mapping scheme is discussed for NPDCCH by utilizing uplink reference signals. The heuristic algorithm proposed in [21] discusses a downlink scheduling mechanism in NB-IoT. In this work, the objective is to efficiently use radio resources in order to support massive connections in the network. In the scheme discussed in [22], narrowband physical downlink shared channel (NPDSCH) subframes are assigned continuously in the radio resource scheduling until a device gets a maximum number of subframes, such that the allocated resources can satisfy the data transmission requirement. The work [11] deals with the enhancement of radio resource utilization for NB-IoT by minimizing the consumption of radio resources during

downlink transmission. However, the dynamic adaptation of MCS and repetition number are not addressed in this work.

Considering the power efficiency of NB-IoT systems, the authors in [23] discuss resource allocation during uplink transmission and analyze the trade-off between power, latency, and rate. The work [24] specifically studies the radio resource allocation with scheduling and computation offloading by focusing on the minimization of the power consumption and average delay in NB-IoT based systems. Although a scheduling is discussed in [25] by considering different coverage classes, latency, and power consumption in NB-IoT, the proposed mechanism does not dynamically adapt the MCS and repetition number during the scheduling. Considering the network slicing in 5G communications, the work [26] addresses the issue of dynamic allocation of resources for different services over a common physical infrastructure. Accordingly, the authors in [26] propose a demand-aware approach for resource allocation in network slicing by combining deep distributional reinforcement learning and GAN.

Therefore, the existing works do not deal with the challenge of intelligent selection of MCS values, repetition numbers, and resources in both uplink and downlink scheduling in NB-IoT. Moreover, the aforesaid parameters have trade-offs, namely when the signal strength is low, the MCS level and number of PRBs need to be decreased but repetitions should be increased. In addition, the selection of these parameters should dynamically cope with different network conditions, considering the constraints (bandwidth, delay, PLR, etc.) of NB-IoT devices and without any prior knowledge of the wireless environment. Consequently, by considering the trade-offs in the MCS, repetitions, and PRB, an online learning based smart technique is required to learn the environment and accordingly, automatically adapt these parameters in parallel.

### B. Our Approach

In this paper, we propose *SmartCon* which is an intelligent adaptation of MCS, repetitions, and PRB during uplink or downlink scheduling, such that the packet loss rate is significantly reduced in NB-IoT networks. In this direction, we design a *Generative Adversarial Network (GAN)* [27] model that uses a deep learning approach to dynamically generate the best suited values for the aforesaid parameters for future scheduling. The proposed GAN considers the variation of signal strength and noise of the channel inputs. In *SmartCon*, the *temporal point process (TPP)* specifies the sequence of time instances of future scheduling (uplink or downlink) associated with the best possible MCS levels, the number of repetitions, and PRBs. To train the GAN, we use a *Multi-Armed Bandit (MAB)* based reinforcement learning mechanism that dynamically tunes its output depending on the impact of the environment. To the best of our knowledge, *SmartCon* is the first work that considers intelligently adapting MCS and repetitions, along with radio resources in NB-IoT systems.

**Reason for applying MAB for generating the training dataset:** The MAB is a reinforcement learning mechanism, where a learning agent opts for a single option (known as *arm*) from a set of available options which have unknown

characteristics at the initial stage. Based on its choice, a certain *reward* is received by the agent. The agent always tries to maximize the cumulative reward. In order to generate the training dataset in our proposed mechanism, each combination of the MCS, repetitions, and PRBs can be considered as an *arm* in the MAB. Therefore, to dynamically select values of the MCS, repetitions, and PRBs, the agent needs to select an *arm* based on the present channel condition such that the packet loss rate will be minimized. Thus, at any time instance, the arm and the associated channel condition can be considered as a state. Therefore, the MAB is a suitable learning model to populate a dataset containing the information related to the intelligent selection of the MCS, repetitions, and PRBs, considering the signal strength of the channel. Consequently, the generated dataset can be used to efficiently train the GAN to dynamically generate the best MCS, repetitions, and PRB values. Moreover, the proposed MAB-based reinforcement learning mechanism helps overcome the lack of diversity in the generated samples in the GAN. The dataset generated by the MAB-based scheme contains values of the MCS, repetitions, and PRBs, which are dynamically selected considering different signal strengths. Thus, in the dataset, the diversity of the samples is maintained by the variation of the channel condition and dynamic adaptation of the aforementioned parameters. Therefore, at the time of the training of the GAN, the generator can generate samples by following the dynamics of the training dataset, and as a consequence, the lack of diversity in the generated samples is overcome.

### C. Contribution of this work

By exploiting online learning, the proposed model can provide an intelligent and unique NB-IoT framework for 5G and B5G networks. The main contributions of this work are summarized as follows:

- 1) We design a GAN-based online learning model for auto link-configuration in NB-IoT. The model generates the real dynamics of the best possible MCS values, repetition numbers, and PRBs. Such dynamic adaptation targets to provide a low packet loss in the network.
- 2) To generate the training dataset, we design a MAB-based reinforcement learning mechanism. It dynamically selects the aforesaid parameters by considering the present channel condition. As a result, a dataset is generated, that contains dynamic adaptation of MCS, repetitions, and PRB, that minimize the packet loss rate in the network. The dataset is then used to train the GAN model.
- 3) For a thorough performance analysis, we implement a prototype of SmartCon in an NB-IoT compatible module of network simulator (NS) version NS-3 i.e., `ns-3-dev-NB-IOT` [28], by extending the LTE medium access control (MAC) [2] module. The results show that SmartCon significantly improves the performance of NB-IoT systems compared to baselines.

### D. Organization of this paper

The remainder of this paper is organized as follows. Section II discusses the formulation of the TPP-based model

to govern the proposed GAN in SmartCon. The details of the proposed GAN model are described in Section III. The MAB-based mechanism used to generate the training dataset is discussed in Section IV. In Section V, the implementation details of SmartCon are presented along with details on the training mechanism. We analyze the performance of SmartCon in Section VI, and Section VII concludes this paper.

## II. TPP-BASED MODEL FORMULATION

In this section, we present the formulation of the TPP-based model that governs the proposed GAN in SmartCon.

### A. Time Series Modeling by Temporal Point Process

A TPP is a stochastic process that contains isolated events at different time-stamps. Formally, a TPP is associated with a series of time-stamps  $\mathcal{T}_t = \{t_l < t | l \in \mathbb{Z}^+\}$ . Here,  $\mathcal{T}_t$  denotes a set of occurrences of events which happened before time  $t$ . In the context of scheduling in NB-IoT, we define  $\mathcal{T}_k(t)$  for eNB  $k$  as the sequence of time instances of scheduling packet transmission (uplink or downlink) associated with the best possible MCS levels, repetition numbers, and the number of PRBs, based on the present channel condition, i.e.,  $\mathcal{T}_k(t) = \{t_l < t | \text{eNB } k \text{ performs scheduling at time } t_l\}$ . Thus,  $\mathcal{T}_k(t)$  is also called the history of scheduling conducted by eNB  $k$  until time  $t$ . In addition,  $\mathcal{T}_k(t)$  can also be expressed as a counting process defined by  $N_k(t) \in \{0\} \cup \mathbb{Z}^+$ , which keeps counting the number of scheduling operations in eNB  $k$  during  $[0, t)$ . If  $u(t-t_l)$  is a Heaviside step function,  $N_k(t)$  can be represented as  $N_k(t) = \sum_{t_l \in \mathcal{T}_k(t)} u(t-t_l)$ .

Given the history  $\mathcal{T}_k(t)$  of scheduling events until time  $t$ , we specify the dynamics of the counting process  $N_k(t)$  using  $\lambda_k(t)$  which captures the conditional probability of scheduling events associated with MCS levels, repetitions, and PRBs, in an infinitesimal time span  $[t, t+dt)$ . Let  $dN_k(t)$  denote the number of such scheduling operations that are initiated by eNB  $k$  in the time interval  $[t, t+dt)$ , and  $dN_k(t)$  be equal to 1. Thus, we have  $\mathbb{P}(dN_k(t) = 1 | \mathcal{T}_k(t)) = \lambda_k(t)dt$ . We consider that scheduling occurrences are independent since the scheduling is influenced by the demand of packet transmission. Thus, we have  $\mathbb{P}(dN_k(t) = n | \mathcal{T}_k(t)) = O(dt) \rightarrow 0 \quad \forall n \geq 2$ . Therefore, scheduling operations are asynchronous. So,  $dN_k(t)$  can be 0 or 1, where  $\lambda_k(t)$  needs to be considered when a scheduling occurs. Thus, we have

$$E[dN(t) | \mathcal{T}_k(t)] = 1 \cdot \lambda_k(t)dt + 0 \cdot (1 - \lambda_k(t)dt) = \lambda_k(t)dt$$

$$\text{i.e. } E[dN(t) | \mathcal{T}_k(t)] = \int_0^T \lambda_k(t)dt. \quad (1)$$

Hence,  $\lambda_k(t)$  also defines the average rate (intensity) of events which are occurring in an infinitesimal interval of time span  $[t, t+dt)$ . So,  $\lambda_k(t)$  is also known as conditional intensity function, which may depend on  $\mathcal{T}_k(t)$ . It is noted that  $\lambda_k(t)$  denotes the stochastic or random dynamics of  $N_k(t)$ .

### B. Why Do We Need to Learn $\lambda_k(t)$ Instead of Applying a Parameterized Model?

Parameterized distributions, such as Hawkes process, Poisson process, cannot capture the effects of various latent factors, such as the variation of signal strength and noise, on the real distribution of  $\lambda_k(t)$ . For instance, the channel condition can affect the rate of packet transmission, while an inappropriate selection of MCS and repetition number can increase the packet loss rate and delay after scheduling. Therefore, by introducing such factors in the distribution of  $\lambda_k(t)$ , we learn the impact of the latent factors during scheduling. Next, we describe the proposed GAN.

### C. The Reason of Applying GAN

Considering the present channel condition, the packet loss rate and delay in the network depend on the MCS, repetitions, and PRBs selection. In our proposed model, the conditional intensity function  $\lambda_k(t)$  represents the distributions of the stochastic time-stamps of traffic scheduling associated with the adaptive MCS, repetitions, and PRBs. In this context, we need to capture the effects of various latent factors (noise, interference, etc.) on the distribution of  $\lambda_k(t)$  to learn the impact of the latent factors during scheduling. Since the GAN can generate the real dynamics by learning the patterns of data in the input dataset, the distribution of  $\lambda_k(t)$  can be smartly modeled using the GAN. Consequently the stochastic time-stamps of traffic scheduling associated with the adaptive values of the aforementioned parameters can be intelligently generated.

## III. SMARTCON: MODELING WITH GAN

The GAN module finds the distribution of  $\lambda_k(t)$  by using the generative and discriminator modules, as shown in Fig. 2.

### A. Generative Module

Let  $\mathbb{K}$  be the set of all eNBs available in the network. For an eNB  $k \in \mathbb{K}$ , time-stamps of scheduling with MCS levels, repetition numbers, and PRBs are governed by the intensity function  $\lambda_k(t)$ , where this conditional intensity function generally depends on the past scheduling operations conducted by eNB  $k$ . We define  $\lambda_k(t)$  as

$$\lambda_k(t) = \Upsilon(\mathcal{T}_k(t); \eta_k(t), \alpha_k(t), \gamma_k(t), \delta_k(t)). \quad (2)$$

Here,  $\Upsilon$  is an arbitrary nonlinear function which is modeled by a recurrent neural network (RNN), where the hidden layers help form recursive units which create an inbuilt memory.  $\eta_k(t)$  is a seed variable or the noise prior, which is a usual input in deep generative models to capture the dynamics of the environment where the model is run. Specifically, in the proposed GAN,  $\eta_k(t)$  introduces a variation of signal strength and noise. Along with  $\eta_k(t)$ , the proposed generative module is provided with three more sources of randomness –  $\alpha_k(t)$ ,  $\gamma_k(t)$ , and  $\delta_k(t)$ . These sources of randomness regulate the dynamics of transmission of the traffic components. All the random sources ( $\eta_k(t)$ ,  $\alpha_k(t)$ ,  $\gamma_k(t)$ , and  $\delta_k(t)$ ) are instantiated only at the time-stamp where a packet is transmitted by the eNB. These random sources are defined as follows:

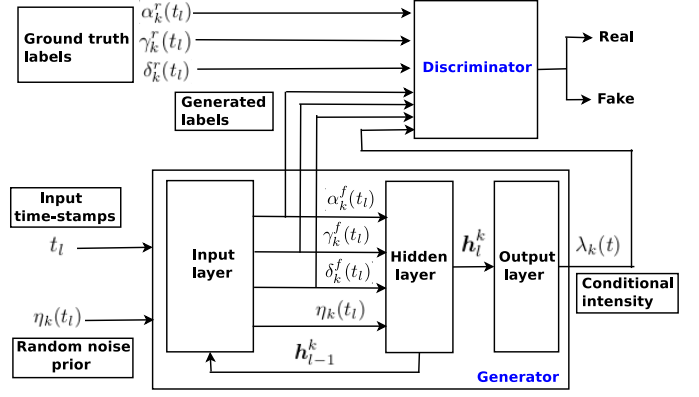


Fig. 2. Generator and discriminator modules in SmartCon

- 1)  $\alpha_k(t)$ :  $\alpha_k \in \{0, 1\}$  is a random variable that identifies the scheduling status of a packet at time  $t$  in eNB  $k$ . When a packet is scheduled for an uplink or downlink transmission, the status is ON ( $\alpha_k(t) = 1$ ); otherwise, the status is OFF ( $\alpha_k(t) = 0$ ).
- 2)  $\gamma_k(t)$ : When the scheduling status is ON for eNB  $k$  (i.e.,  $\alpha_k(t) = 1$ ), the number of PRBs used to transmit the packets scheduled at  $t$  is determined by  $\gamma_k(t)$ . More specifically,  $\gamma_k(t) \in [0, 1]$  stores normalized values of the number of PRBs at time  $t$  in eNB  $k$ .
- 3)  $\delta_k(t)$ : This parameter is a pair of normalized values of MCS and repetition number, which are associated with the scheduling of a packet at time  $t$  in eNB  $k$ . The value of  $\delta_k(t)$  is defined when the scheduling status is ON i.e.,  $\alpha_k(t) = 1$ .

In the RNN, recursive units help create an inbuilt memory, and thus the impacts of the past transmissions on the present transmission can be captured correctly. The proposed GAN uses one RNN ( $RNN_k$ ) per eNB  $k$ .  $RNN_k$  considers the previous time-stamps ( $t_l \in \mathcal{T}_k(t)$ ) of scheduling packet transmissions associated with MCS levels, repetitions, and radio resources as inputs and generates the conditional intensity function  $\lambda_k(t)$  for the scheduling events of the next packets. In this context, the hidden states of  $RNN_k$  embed the history  $\mathcal{T}_k(t)$  into the vectors  $\mathbf{h}_l^k$  which are determined recursively by utilizing the previous information  $\mathbf{h}_{l-1}^k$  and the signals acquired from the present input. For eNB  $k$ , such  $\mathbf{h}_l^k$  are fixed low dimensional representations of the history of scheduled packets associated with a MCS, repetition number, and number of PRBs. Fig. 2 illustrates different parameters used in the generator, along with the discriminator module. In the generator, the RNN has three layers as follows.

1) *Input layer*: The activation of the input layer occurs when a packet is transmitted. Specifically, at the  $l$ -th transmission time ( $t_l$ ), the input layer considers the previous states  $\mathbf{h}_{l-1}^k$  as input and produces the random signals  $\eta_k(t_l)$ ,  $\alpha_k(t_l)$ ,  $\gamma_k(t_l)$ , and  $\delta_k(t_l)$ , which are fed into the next layer (the hidden layer). Particularly, at time-stamp  $l \geq 1$ , the input layer creates the aforesaid random signals as follows.

- **Definition of  $\eta_k(t_l)$** : At time-stamp  $t_l$ , a Poisson distribution is used to generate the noise prior, i.e.,  $\eta_k(t_l) \sim$

Poisson( $\mu$ ), where  $\mu \geq 0$  is average number of occurrences of events per interval.

- **Definition of  $\alpha_k(t_l)$ :** The random variable,  $\alpha_k(t_l)$ , which decides whether packet scheduling is ON/OFF is sampled from a Bernoulli distribution. The mean of this distribution is represented by a logistic function of the preceding hidden state  $\mathbf{h}_{l-1}^k$ . That is,

$$\alpha_k(t_l) = \text{Bernoulli}(\xi_k(t_l)), \quad (3)$$

where  $\xi_p(t_l) = \sigma(\mathbf{w}_\alpha^T \mathbf{h}_{l-1}^k)$ . Here,  $\mathbf{h}_{l-1}^k$  is the output of the hidden layer, which represents the state of the RNN at time-stamp  $t_{l-1}$ . When  $\mathbf{h}_0^k = 0$ ,  $\alpha_k(t_l) = \text{Bernoulli}(1/2)$ .

- **Definition of  $\gamma_k(t_l)$ :** The density function of  $\gamma_k(t_l)$  depends on the noise  $\eta_k(t_l)$ , and thus  $\gamma_k(t_l)$  is defined using a standard normal distribution, as follows.

$$\gamma_k(t_l) = \frac{1}{\sqrt{2\pi}} \exp\left(-\frac{(\eta_k(t_l))^2}{2}\right) \quad (4)$$

- **Definition of  $\delta_k(t_l)$ :** In eNB  $k$ , at time-stamp  $t_l$ , let  $m_k(t_l)$  and  $r_k(t_l)$  be random variables that represent the MCS and repetition number, respectively. Since the selection of MCS values and repetition numbers is influenced by  $\eta_k(t_l)$ ,  $m_k(t_l)$  and  $r_k(t_l)$  are defined as

$$\mathbb{P}(m_k(t_l) | \alpha_k(t_l) = 1) = \frac{\beta \exp(-\beta \eta_k(t_l))}{1 - \exp(-\beta)}, \quad (5)$$

$$\mathbb{P}(r_k(t_l) | \alpha_k(t_l) = 1) = \beta \exp(-\beta \eta_k(t_l)). \quad (6)$$

Eqns. (5) and (6) indicate that  $m_k(t_l)$  and  $r_k(t_l)$  follow exponential distributions and take values between  $[0, 1]$ . Eqns. (5) and (6) allow us to generate random variables that follow the exponential distribution and depend on another random variable. Since  $\eta_k(t)$  introduces a variation in signal strength and noise, the MCS  $m_k(t_l)$  and repetition number  $r_k(t_l)$  depend on  $\eta_k(t)$ , and therefore  $m_k(t_l)$  and  $r_k(t_l)$  are calculated using Eqns. (5) and (6). In this context, we consider exponential distributions for  $m_k(t_l)$  and  $r_k(t_l)$  because their impacts on the network performance are significantly influenced by the variation of signal strength and noise. In Eqns. (5) and (6), a difference is added to the denominator to impose a variation between the values of  $m_k(t_l)$  and  $r_k(t_l)$ . The MCS and repetition number are selected when a packet is scheduled, and therefore values of the MCS and repetition number are defined when  $\alpha_k(t_l) = 1$ . The functional forms of Eqns. (5) and (6) are borrowed from [29]. In Eqns. (5) and (6),  $\beta > 0$ . Since  $\delta_k(t_l)$  is a pair of values, we define  $\delta_k(t_l)$  as  $\delta_k(t_l) = \{m_k(t_l), r_k(t_l)\}$ . When  $\alpha_k(t_l) = 0$ , scheduling is not performed. Thus,  $\delta_k(t_l) = 0$  is deterministic when  $\alpha_k(t_l) = 0$ . Therefore, we have

$$\mathbb{P}(\delta_k(t_l) | \alpha_k(t_l) = 0) = \text{Dirac delta}(\delta_k(t_l)). \quad (7)$$

The functional form of Eqn. (7) is borrowed from [29].

2) *Hidden layer:* The input time-stamps  $t_l$  and the random signals produced in the previous layer are used to create the next state  $\mathbf{h}_l^k$  based on the present hidden state  $\mathbf{h}_{l-1}^k$ . The definition of  $\mathbf{h}_l^k$  is

$$\mathbf{h}_l^k = \Omega_g \left( \mathbf{W}_1 \mathbf{h}_{l-1}^k + \mathbf{W}_2 \alpha_k(t_l) (\gamma_k(t_l) + \delta_k(t_l)) + \mathbf{W}_3 (1 - \alpha_k(t_l)) t_l \eta_k(t_l) + \mathbf{b}_h \right). \quad (8)$$

Here,  $\Omega_g$  is an activation function, and  $\mathbf{W}_1$ ,  $\mathbf{W}_2$ ,  $\mathbf{W}_3$  and  $\mathbf{b}_h$  are trainable parameters.  $\Omega_g$  uses the *Rectified Linear Unit (ReLU)* activation function, which requires less computations than other activation functions. To overcome the vanishing gradient problem, we use the *Rectified Linear Unit (ReLU)* as the activation function in the hidden layers [30]. The ReLU does not cause a small derivative. When the value of the input variable is greater than 0, the gradient of the ReLU is 1, and zero otherwise. Therefore, multiplying a set of ReLU derivatives in the backpropagation equations results in 0 or 1, and consequently, there is no ‘vanishing’ of the gradient.

Note that the proposed model is stateful, which is a key distinguishing characteristic. Normalized values of the number of PRBs, MCS and repetition number need to be considered when a packet is scheduled for uplink or downlink transmission, i.e., the value of  $\alpha_k(t_l)$  is 1. Thus, in Eqn. (8),  $\gamma_k(t_l)$  and  $\delta_k(t_l)$  are multiplied by  $\alpha_k(t_l)$ , along with the trainable parameter  $\mathbf{W}_2$ . When packet scheduling is not performed, the MCS and repetition number are not required, and therefore only the noise value is considered with the time instant. This scenario is represented by the term  $\mathbf{W}_3 (1 - \alpha_k(t_l)) t_l \eta_k(t_l)$ , with the trainable parameter  $\mathbf{W}_3$ .

3) *Output layer:* Based on the hidden states, the output layer generates the conditional intensity  $\lambda_k(t)$  as

$$\lambda_k(t) = \exp(\mathbf{W}_g^T \mathbf{h}_l^k + \mathbf{c}_g(t - t_l) + \mathbf{b}_g). \quad (9)$$

Here,  $t_l < t$  and  $\lambda_k(t)$  samples the next time-stamp by applying Ogata’s thinning algorithm [31]. Let  $\theta_G = \{\mathbf{W}_1, \mathbf{W}_2, \mathbf{W}_3, \mathbf{b}_h, \mathbf{W}_g, \mathbf{c}_g, \mathbf{b}_g\}$  be trainable parameters used in the generative model. Under the generative framework, the log-likelihood of  $\lambda_k(t)$  can be defined as

$$\log \mathcal{L}(\lambda_k | \theta_G) = \sum_{j=1}^{|\mathcal{H}(T)|} \log \lambda_k(t_j) - \int_0^T \lambda_k(t) dt. \quad (10)$$

## B. Discriminative Module

In general, let  $\alpha_k^*(t_l)$ ,  $\gamma_k^*(t_l)$ , and  $\delta_k^*(t_l)$  be the values fed into the discriminator, which may be fake or real. The discriminative unit takes a series  $F$  of fake data generated by the generative module and a series  $R$  of real (observed) values for  $F$ . Specifically, we represent  $F$  and  $R$  as  $F = (\alpha_k^f(t_l), \gamma_k^f(t_l), \delta_k^f(t_l))$  and  $R = (\alpha_k^r(t_l), \gamma_k^r(t_l), \delta_k^r(t_l))$ . We design the discriminator using an RNN whose hidden layer for eNB  $k$  at time  $t_l$  is defined in what follows.

$$\Phi_l^k(\alpha_k^*(t_l), \gamma_k^*(t_l), \delta_k^*(t_l)) = \Omega_d \left( \mathbf{W}_4 \Phi_{l-1}^k + \mathbf{W}_5 (\alpha_k^*(t_l) + \alpha_k^*(t_l) \gamma_k^*(t_l) \delta_k^*(t_l)) + \mathbf{b}_d \right) \quad (11)$$

At each time  $t_l$ , the hidden layer of the discriminative model outputs  $\Phi_l^k$ , which defines the probability of correctness of  $\alpha_k^*(t_l)$ ,  $\gamma_k^*(t_l)$ , and  $\delta_k^*(t_l)$ , i.e., if they belong to  $R$ . In Eqn. (11),  $\Omega_d$  is the sigmoid activation function. From (11), it is noted that  $\gamma_k^*(t_l)$  and  $\delta_k^*(t_l)$  have no effect when  $\alpha_k^*(t_l)$  is zero. This protects against noise in the input data, where  $\gamma_k^*(t_l)$  and  $\delta_k^*(t_l)$  are non-zero while  $\alpha_k^*(t_l)$  is zero. Assume that  $\theta_D = \{\mathbf{W}_4, \mathbf{W}_5, \mathbf{b}_d\}$  are the trainable parameters for the discriminator. In case of real sequence  $R$ , the log-likelihood of the discriminator (expected value of  $\log D_{\theta_D}$ ) is defined as

$$E_{R, \theta_D}[\log D_{\theta_D}] = \sum_{j=1}^{|R|} \log \Phi_l^k(\alpha_k^r(t_l), \gamma_k^r(t_l), \delta_k^r(t_l)). \quad (12)$$

For a fake sequence ( $F$ ), the log-likelihood of the discriminator is

$$E_{R, \theta_G, \theta_D}[\log(1 - D_{\theta_D})] = \sum_{j=1}^{|F|} \log \left( 1 - \Phi_l^k(\alpha_k^f(t_l), \gamma_k^f(t_l), \delta_k^f(t_l)) \right). \quad (13)$$

Now, in SmartCon, the loss function of the proposed GAN model is defined as

$$\min_{\theta_G} \max_{\theta_D} -\log \mathcal{L}(\lambda_k | \theta_G) + E_{R, \theta_D}[\log D_{\theta_D}] + E_{R, \theta_G, \theta_D}[\log(1 - D_{\theta_D})]. \quad (14)$$

Therefore, SmartCon maximizes the log-likelihood of the conditional intensity  $\lambda_k$  and optimizes the adversarial objective for generating the labels ( $\alpha_k^*(t_l)$ ,  $\gamma_k^*(t_l)$ , and  $\delta_k^*(t_l)$ ). At a time, only one data sample is processed in the stochastic gradient descent (SGD), and thus the SGD is computationally fast. In addition, since the SGD causes more frequent updates to the parameters, it has faster convergence for larger datasets [32]. Therefore, the SGD is used to solve the optimization problem in Eqn. (14).

### C. Learning with GAN

Once the GAN model can generate the real labels' dynamics ( $\alpha_k^*(t_l)$ ,  $\gamma_k^*(t_l)$ , and  $\delta_k^*(t_l)$ ), SmartCon performs the predictions described in what follows.

- Based on  $\alpha_k^*(t_l)$ , the eNB predicts the probability of packet scheduling at time  $t_l$ .
- Based on  $\gamma_k^*(t_l)$ , the required number of PRBs for the scheduling is chosen.
- Based on  $\delta_k^*(t_l)$ , eNB  $k$  selects the best possible MCS level and repetition number for the scheduling at  $t_l$ .

In particular, the GAN does not belong to the traditional reinforcement learning model. However, considering a reinforcement learning approach, the proposed GAN has three states – (i) the generation of  $\alpha_k^f(t_l)$ ,  $\gamma_k^f(t_l)$ , and  $\delta_k^f(t_l)$ , by the generator, (ii) the generation of  $\lambda_k(t)$  by the generator, and (iii) the differentiation between the fake and real values of  $\alpha_k(t_l)$ ,  $\gamma_k(t_l)$ , and  $\delta_k(t_l)$ , by the discriminator. The optimization function in Eqn. (14) can be considered as the *reward*. The action space can be defined as a set of actions that transfer the data produced in a state to another state of the GAN.

## IV. TRAINING DATASET GENERATION

In this section, we present our MAB-based [33] dynamic selection of MCS, repetitions, and radio resources, in order to prepare the training dataset. Specifically, the  $\epsilon$ -greedy algorithm which is a variant of MAB mechanism is used in our proposed mechanism.

### A. $\epsilon$ -greedy Algorithm

We use  $\epsilon$ -greedy policy [34] as a MAB mechanism to dynamically select the MCS and repetition number given the present signal-to-interference-plus-noise ratio (SINR) value of the channel. The  $\epsilon$ -greedy mechanism uses a parameter  $\epsilon$  as exploration probability. At time instant  $t$ ,  $\epsilon_t$  is defined as  $\epsilon_t = \min(1, cK/d^2t)$ . Here,  $K$  is the total number of arms used in the bandit problem. The parameter  $c \geq 0$  is a small integer. The parameter  $d$  specifies the difference between the expected rewards of the best and second best arms. Here, the best arm denotes the arm that has provided the maximum average reward so far. The  $\epsilon$ -greedy policy is described by two phases listed below.

- **Exploration:** In the exploration phase, we randomly choose an arm from the available set of arms. The probability of exploration is defined by  $\epsilon$ .
- **Exploitation:** In the exploitation phase, we choose the arm associated with the maximum average reward so far. In this case,  $(1-\epsilon)$  defines the probability of exploitation.

In [35], it is described that after  $n$  number of plays, the probability of choosing a suboptimal arm is upper bounded by  $O(c/d^2n)$ , where  $n \geq cK/d^2$ .

### B. Exploiting MAB for Dynamic Selection of MCS and Repetition Number

Let  $\mathcal{M}$  be the set of available MCS values,  $\mathcal{R}$  the set of available repetition numbers, and  $\mathcal{P}$  the set of number of PRBs available in NB-IoT systems. Let  $\mathcal{M} = \{M_1, M_2, M_3, \dots, M_p\}$ ,  $\mathcal{R} = \{R_1, R_2, R_3, \dots, R_q\}$ , and  $\mathcal{P} = \{P_1, P_2, P_3, \dots, P_u\}$ , where  $p > 0$ ,  $q > 0$ , and  $u > 0$  are the counts of the available MCS values, repetitions, and PRBs, respectively. In our MAB model, the selection of MCS levels, repetitions, and number of PRBs is the *arm* and we refer to it as *MCS-Repetition-PRB (M-R-P) configuration*. Let  $\mathcal{A}$  be the arm, and therefore the arm with  $a^{th}$  MCS value,  $b^{th}$  repetition number, and  $c^{th}$  number of PRBs can be represented as  $\mathcal{A}_{abc} = \{M_a, R_b, P_c\}$ , where  $1 \leq a \leq p$ ,  $1 \leq b \leq q$  and  $1 \leq c \leq u$ . Thus,  $K$  specifies the total count of  $\mathcal{A}_{abc}$ . In the dynamic selection of MCS values, repetitions, and PRBs, the objective is to minimize the packet loss rate after scheduling. Thus, in our MAB model, the reward is the inverse of the PLR and let  $\mathcal{D}$  denote PLR.

1) *Statistic table:* We use a statistic table, denoted by  $\mathbb{S} = \{\mathcal{S}, \mathcal{A}, \mathcal{D}\}$ , in order to store information regarding the selected M-R-P configuration for the present SINR of the channel.  $\mathbb{S}$  also stores the PLR observed against the values of aforesaid selected parameters.  $\mathcal{S}$  denotes the SINR of the channel.

---

**Algorithm 1** MAB-based Selection of MCS Levels, Repetitions and PRBs
 

---

```

1: Start
2: Initial stage: Calculate the present SINR  $S_t$  of the channel and select the M-R-P
   configuration randomly from the set of available configurations. After a time period
    $t_d$ , compute the packet loss rate.
3: Experience stage: At time  $t$ , calculate the present  $S_t$ .
4: Calculate  $\epsilon_t$  by using  $\epsilon_t = \min(1, cK/d^2t)$ .
5: Let  $\zeta \leftarrow \text{Random}(0,1)$ .
6: if  $\zeta \leq \epsilon_t$  then
7:   if  $S_t \in [(S_t - \Delta), (S_t + \Delta)]$  in  $\mathbb{S}^S \subset \mathbb{S}$  then
8:     Choose M-R-P configuration  $\mathcal{A}_t$  from  $\mathbb{S}^S$  such that  $\mathcal{A}_t$  provides the lowest
     PLR (i.e.  $\mathcal{D}$ ) in  $\mathbb{S}^S$ .
9:   else
10:    Select M-R-P configuration  $\mathcal{A}_t$  from  $\mathbb{S}$  such that  $\mathcal{A}_t$  provides the lowest
    PLR in  $\mathbb{S}$ .
11:   end if
12: else
13:   Choose an M-R-P configuration at random from the available set of M-R-P
   configurations.
14: end if
15:  $\mathcal{D}$  is calculated.
16:  $\mathbb{S}$  is updated with  $\mathcal{S}$ ,  $\mathcal{A}$ , and  $\mathcal{D}$ .
17: End

```

---

2) *Execution of the MAB Approach:* In Algorithm 1, there are two stages – (1) *initial stage*, and (2) *experience stage*. Descriptions of these two stages are given in what follows.

(1) **Initial stage:** The learning agent  $\mathcal{L}$  calculates the SINR of the channel and selects the M-R-P configuration randomly from the set of available configurations. After a time period of  $t_d$ ,  $\mathcal{L}$  calculates the PLR and computes the reward accordingly. Therefore, the initial stage helps the agent populate  $\mathbb{S}$  to start the experience stage.

(2) **Experience stage:** The description of the exploitation is as follows.

**Exploitation:** At time  $t$ , let the SINR be  $S_t$  and the exploitation be executed with probability  $(1 - \epsilon_t)$ . We consider two scenarios as follows.

- 1) **Case-1** (*Consideration of a subset of  $\mathbb{S}$ :*) This case allows the exploitation of past knowledge to select the best M-R-P configuration for the present SINR. In this context, a small value  $\Delta > 0$  is chosen to define the range of the SINR in  $\mathbb{S}$ , where the present SINR is found. Hence, specifically, *Case-1* can be defined as follows. If  $S_t \in [(S_t - \Delta), (S_t + \Delta)]$  in  $\mathbb{S}^S \subset \mathbb{S}$ , the M-R-P configuration  $\mathcal{A}_t$  is chosen from  $\mathbb{S}^S$  such that  $\mathcal{A}_t$  provides the lowest PLR in the set  $\mathbb{S}^S$ .
- 2) **Case-2** (*Consideration of the entire  $\mathbb{S}$ :*) The second case uses the best past experience without considering the present SINR since it is not found in the range of the SINR defined by  $\Delta$  in  $\mathbb{S}$ . Particularly, *Case-2* is defined as follows. If  $S_t \notin [(S_t - \Delta), (S_t + \Delta)]$  in  $\mathbb{S}$ , the M-R-P configuration  $\mathcal{A}_t$  is chosen from the entire  $\mathbb{S}$  such that  $\mathcal{A}_t$  provides the lowest PLR in  $\mathbb{S}$ .

**Exploration:** An M-R-P configuration is selected randomly with probability  $\epsilon_t$  from the M-R-P configuration.

## V. IMPLEMENTATION AND TRAINING DETAILS

We implement SmartCon in `ns-3-dev-NB-IOT` [28] with one eNB, where the number of UEs is varied from 10 to 100. The NB-IoT module belongs to LTE Cat NB1, where the downlink and uplink peak data rates are 26 kbps and 66 kbps, respectively. Both uplink and downlink transmissions are

TABLE I  
SIMULATION PARAMETERS

Parameter	Value
Frequency Band	DL: 925 MHz, UL: 880 MHz
Default Transmission Mode	0 (Single-input-single-output (SISO))
Path loss model	FriisSpectrumPropagationLossModel
Fading model	TraceFadingLossModel
Propagation model	Okumura-Hata (Open area), Hybrid building(Urban)
NoiseFigure of UE	5 dB
NoiseFigure of eNB	9 dB
Downlink peak data rate	26 kbps
Uplink peak data rate	66 kbps
Propagation delay model	Constant speed propagation delay model
Bit error rate (BER)	0.03
UE scheduler type	PfFfMacScheduler
Packet Size	100 bytes
Mobility model	Random direction 2d mobility model ("Bounds: Rectangle (-100, 100, -100, 100)", "Speed: ConstantRandomVariable [Constant=3.0]", "Pause: ConstantRandomVariable [Constant=0.4]")
System bandwidth	180 kHz
TxPower of UE	23 dBm
TxPower of eNB	46 dBm
Cell radius	1.5 km
Transmission mode	Multi-Tone
Receiver Chains	1 SISO
Number of Antennas	1
Duplex Mode	Half duplex

considered. The NB-IoT module in NS-3 includes numerous features, such as radio resource control (RRC), radio link control (RLC), packet scheduling, physical layer error model, inter-cell interference coordination, dynamic spectrum access, etc. [5], [14]. We have used these aspects in the implementation of our proposed mechanism. We vary the levels of the interference in order to analyze the performance of SmartCon in different channel conditions. We consider both UDP and TCP packets with a ratio of 80% and 20%, respectively. We use *proportional fair scheduling* to schedule the packets. The UEs are placed following a Poisson distribution centered at the eNB's position. To set the MCS, TBS, PRB, and code rate for a channel condition, we have applied the standard tables defined by the 3GPP standard [3]. Unless stated otherwise, we set the number of UEs to 100. The SINR is chosen randomly between 5dB–25dB. Details on the simulation setup are given in Table I.

### A. Baseline Mechanisms

We have considered NANIS [11] and NBLA [12] as baselines along with the standard scheduling approach in NB-IoT. NANIS addresses the adaptation problem of the time interval between two consecutive NPDCCHs. NBLA is a threshold-based approach, where an uplink link adaptation is performed with the determination of the MCS value and repetition number. The standard approach is basically a First-In First-Out (FIFO) mechanism with a static MCS value and no repetition number. Here, we set the MCS to 6. We also compare the performance of SmartCon with GAN-powered deep distributional Q network (GAN-DDQN) to add a comparison with a mechanism that combines the GAN and reinforcement learning. However, the GAN-DDQN is a dynamic allocation mechanism of network slicing resources in 5G communications.

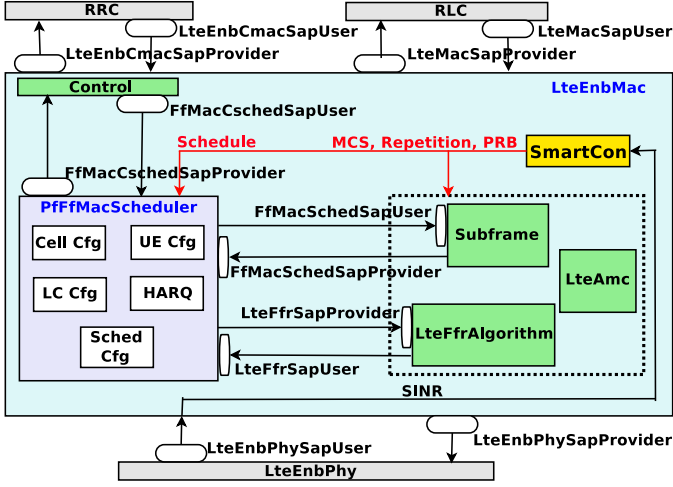


Fig. 3. SmartCon implementation modules in ns-3-dev-NB-IOT

### B. Implementation of SmartCon

We have implemented SmartCon by extending the LTE MAC [2] module of ns-3-dev-NB-IOT, as shown in Fig. 3. The OnOffApplication is used to generate the traffic. The MAC layer functionalities of the eNB are implemented by the class LteEnbMac and PfffMacScheduler implements the *proportional fair scheduler* to perform scheduling of UEs. In LteEnbMac, there are five interfaces for handling subframe, control information, packet scheduling (uplink and downlink), MCS assignment, and PRB allocation, implemented by a subframe block, control block, scheduler block, LteAmc, and LteFfrAlgorithm, respectively. Specifically, LteFfrAlgorithm is the base class that allocates PRBs and subframes for the transmission of data using a frequency reuse algorithm. We implement SmartCon as an extension to the LteEnbMac. The LteEnbPhy interface reports the SINR of the channel to LteEnbMac, where the SINR is utilized by SmartCon. It uses the subframe block, LteAmc, and LteFfrAlgorithm interfaces to assign subframes with PRBs, MCS, and repetition numbers.

### C. Implementation of Repetitions

Whenever repetition is applied, the successive repetitions of the packets are aggregated at the eNB. We have modified the functionality of the physical layer to incorporate the aggregation of all the repetitions.

### D. Training Environment Setup

For the training setup, the network has three eNBs and each cell has 50 UEs randomly located inside a cell. We randomly choose the run time for each simulation instance between 100-500 seconds. The number for runs of each simulation instance is also selected randomly between 60-120, and both downlink and uplink transmissions are considered in every simulation instance. The SINR value is selected randomly between 20dB-45dB and the per-frame SINR is reported by the LteEnbMac interface. The collected data includes the time-stamped packet scheduling (uplink and downlink) events, SINR of the channel,

the selected MCS and repetition number, the number of PRBs used for the transmission, and the packet loss rate. The total size of the dataset is close to 2 GB.

### E. Training of the Model

To generate the data for the dataset, we use the following information – (i) uplink and downlink scheduling time-stamps, (ii) SINR of the channel, (iii) MCS and repetition number selected for data transmission, (iv) number of PRBs used for the transmission, and (v) average packet loss rate after the transmission. All this data is represented as a time series. The training dataset contains information related to the scheduling events, and the selection of the PRBs, MCS, and repetitions. In the dataset, the first parameter identifies the scheduling status of a packet. When a packet is scheduled for an uplink or downlink transmission, the status is ON; otherwise, the status is OFF. When the scheduling status is ON, the number of PRBs used to transmit the packets is determined by the second parameter. The third parameter is the pair of MCS and repetition numbers, which are associated with the scheduling of packets, and thus the third parameter is defined when the scheduling status is ON.

In particular, the dataset used to train the GAN contains  $\alpha_k^r(t_l)$ ,  $\gamma_k^r(t_l)$ , and  $\delta_k^r(t_l)$ . Since  $\gamma_k^r(t_l)$  stores the normalized value of the number of PRBs and  $\delta_k^r(t_l)$  represents the normalized values of the MCS and repetition number, we need to normalize the number of PRBs, MCS value, and repetition number between  $[0, 1]$ . For instance, the MCS value is normalized between  $[0, 1]$  using  $(x - MCS_{min}) / (MCS_{max} - MCS_{min})$ . In this case,  $x$  is considered as the MCS value selected at any time instant. Here,  $MCS_{min}$  and  $MCS_{max}$  denote the minimum and maximum MCS values in NB-IoT, respectively, where  $MCS_{min} = 0$  and  $MCS_{max} = 12$ .

After generating the training dataset, the GAN is trained, tested, and validated using 60%, 20%, and 20% of the dataset, respectively. We have applied a 10-fold cross-validation technique with randomly chosen validation sets to evaluate the predictive model. In case of the convergence of the GAN, the losses of the discriminator and generator become quite stable after approximately 2200 epochs. After evaluating the predictive model, all the eNBs are loaded with the trained model. Then, the MAB model is again run to collect the same aforesaid information which is used to retrain the GAN model.

### F. Prediction Performance

To calculate the accuracy of the predictions of the GAN model, we measure the Mean Absolute Percentage Error (MAPE) [36]. MAPE is a continual-time metric that computes the mean absolute deviation between the actual values and the predicted values of the number of PRBs, MCS, repetition number, and probability of scheduling, up to the present time-stamp. We compute the average MAPE value ( $MAPE_{avg}$ ) of these parameters. We have observed that, for the test data, the  $MAPE_{avg}$  of the GAN model is 5.21% which signifies that the error of the trained model is quite low.

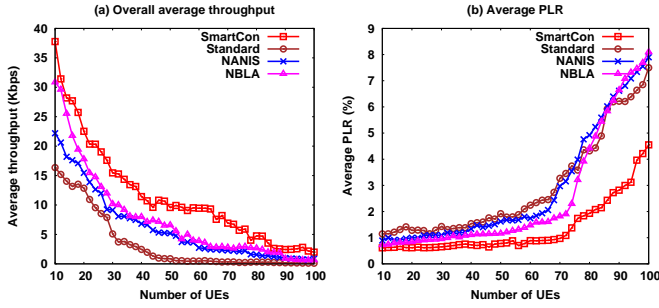


Fig. 4. (a) Average throughput and (b) Average packet loss rate

### G. Model Size Optimization

Table II summarizes the observations including the model size and MAPE values ( $MAPE_{avg}$  values) for different training data sizes. From this table, it is noted that 60% of the data from the collected dataset provides a  $MAPE_{avg}$  value of 5.83% with a trained model size of 47.3 MB. This  $MAPE_{avg}$  is quite acceptable and is associated with a low trained model size (47.3 MB). Therefore, we select 60% of the data from the collected dataset to choose our optimal model size. This trained model is loaded in the eNB for online prediction during the execution of SmartCon.

TABLE II  
MODEL SIZE AND  $MAPE_{avg}$  FOR DIFFERENT TRAINING DATA SIZES

Training data size	30%	40%	50%	60%	70%	80%
$MAPE_{avg}$	23.8%	11.4%	8.56%	5.83%	5.34%	4.97%
Model size (MB)	36.2	41.6	44.8	47.3	76.1	129.5

### H. Model Retraining

Whenever a packet loss occurs, SmartCon finds out the correlation between the average packet loss rates in the past execution of duration (window)  $\rho$  and the pre-loaded training sample chosen randomly. If this correlation is low, SmartCon sends a signal to the eNB, which signifies that a new sample dataset has been prepared over a window  $\rho$ . In the implementation,  $\rho$  is set to 1 minute, and the new dataset's size should be of 2 GB in order to update the trained model.

### I. The Core Module

The core functionality of SmartCon is to emulate the GAN model on the basis of Ogata's thinning algorithm [31]. We run SmartCon once in each window  $\rho$ .

## VI. PERFORMANCE ANALYSIS

We run each simulation instance for 500 seconds, where the results are shown as an average of 100 runs of each simulation instance. Every simulation instance is a combination of downlink and uplink transmissions.

### A. Analysis of Throughput

In SmartCon, the generated dynamics lead to the adaptive selection of PRB, MCS, and repetitions in future scheduling. This learning-based adaptability helps tune the aforesaid parameters based on the present channel condition, such that

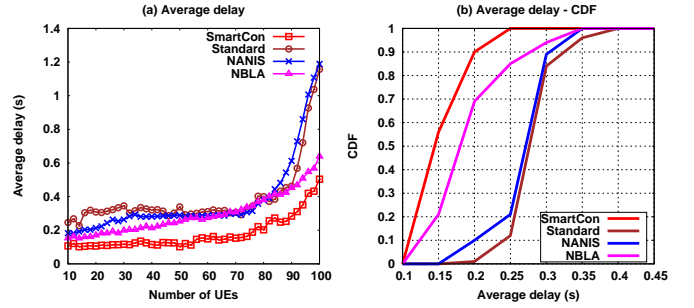


Fig. 5. (a) Average packet delay and (b) Average packet delay distribution

the average throughput is significantly enhanced. For instance, a higher number of repetitions is chosen when the channel condition is poor so that the transmitted data can reach the destination. Since NBLA is based on threshold-based scheme to adapt the MCS and repetitions, the adaptation is not as efficient as our proposed online learning mechanism. Whereas, since NANIS and the standard approaches do not dynamically deal with the selection of MCS and repetitions, values of these parameters cannot be adaptively tuned in different channel conditions. Therefore, the average throughput is significantly lower in the baselines compared to SmartCon. Fig. 4(a) indicates that, SmartCon has approximately 18, 2.2, and 3 times higher average throughputs than the standard, NANIS, and NBLA schemes, respectively.

### B. Analysis of Packet Loss Rate

In the generated dataset, the MCS, number of PRBs, and repetition number are chosen to minimize the packet loss rate. In this regard, the application of the best possible value of MCS plays a key role, where a low MCS level should be chosen when the channel condition is poor. Otherwise, the packet loss rate increases. Fig. 4(b) shows that SmartCon has a significantly lower PLR than other baseline mechanisms. When the number of UEs is 50, the average PLR in SmartCon is approximately 59%, 52%, and 33% lower than the standard, NANIS, and NBLA approaches, respectively. However, as the number of UEs increases in the network, the adaptability of NANIS and NBLA decreases, as illustrated in Fig. 4(b).

### C. Analysis of Packet Delay

In SmartCon, the unnecessary use of repetitions in a transmission helps reduce the time for a packet to reach its destination. Based on the present channel condition, the selection of the best MCS value provides the best possible data rate, and consequently the transmission delay is decreased. From Fig. 5(a), it can be noted that SmartCon has approximately 56%, 58%, and 21% lower average packet delay than the standard, NANIS, and NBLA schemes, respectively. Fig. 5(b) illustrates the cumulative distribution function (CDF) of the average packet delay, where the distribution in SmartCon is concentrated in the 0.1–0.25s range. NBLA provides a higher distribution of average delay (0.1 – 0.35s) than SmartCon, as shown in Fig. 5(b). Whereas, the other baselines have significantly higher average delay CDF (up to 0.4s).

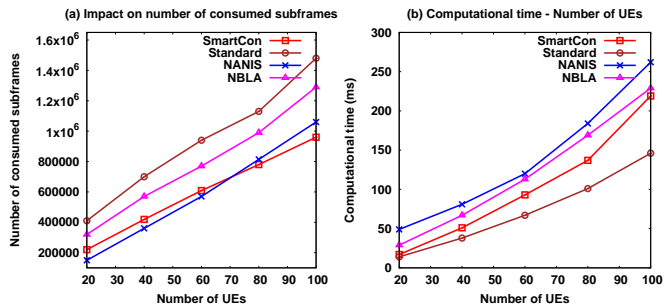


Fig. 6. (a) Number of consumed subframes and (b) Computational time

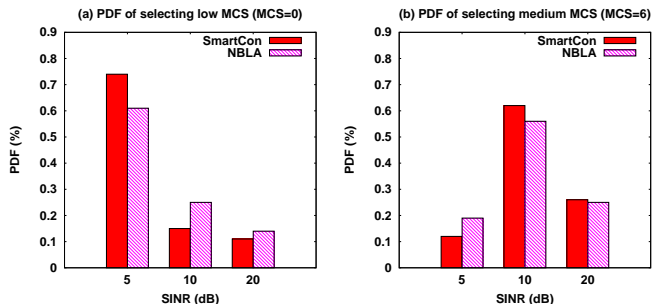


Fig. 7. Distribution of the selection of: (a) Low MCS (MCS=0) and (b) Medium MCS (MCS=6)

#### D. Analysis of the Number of Consumed Subframes

In the proposed mechanism, the learning is based on the training with a large number of UEs, where the number of sufficient subframes is dynamically adjusted to minimize the PLR. Therefore, based on the training, SmartCon becomes intelligent to appropriately select the number of subframes in different network scenarios having different number of UEs. As a result, from Fig. 6(a), it can be observed that SmartCon has a consumption of subframes approximately 35%, 9%, and 26% lower than the standard, NANIS, and NBLA schemes, respectively.

#### E. Analysis of Computational Time

In SmartCon, after the training phase, the GAN model simply generates the future dynamics for a UE in the execution phase, which does not depend on any database or set of computations as required in NANIS and NBLA. Therefore, SmartCon has a lower computational time (Fig. 6(b)). When the number of UEs is 100, SmartCon requires approximately 11%, and 4% lower computational time than NANIS, and NBLA, respectively. Meanwhile, when the number of UEs is 50, in SmartCon, the computational time is approximately 16% lower than NANIS.

#### F. Analysis of Selection of MCS Levels

Since a higher MCS value increases the PLR in case of low signal strength, the tendency of SmartCon is to decrease the MCS level as the signal strength of the channel deteriorates and vice versa, as illustrated in Figs. 7 and 8(a). In our baseline mechanisms, only NBLA adapts the MCS and repetitions, and therefore we consider only NBLA in the analysis of MCS

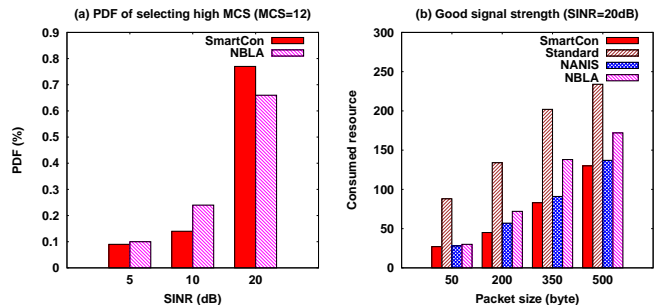


Fig. 8. (a) Distribution of the selection of high MCS (MCS=12) and (b) Consumed resources under high signal strength (SINR=20dB)

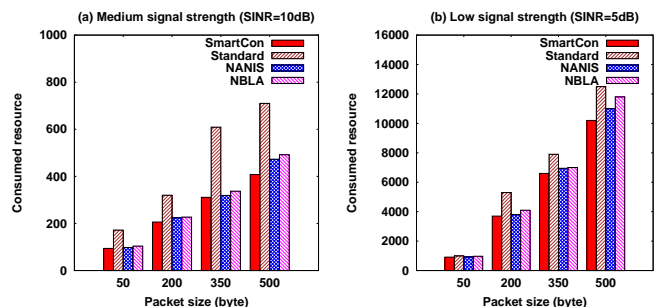


Fig. 9. (a) Consumed resources under medium signal strength (SINR=10dB) and (b) Consumed resources under low signal strength (SINR=5dB)

selection. Table III presents a comparative analysis of the probability density function (PDF) of the MCS selection in SmartCon and NBLA.

TABLE III  
ANALYSIS OF THE PDF OF MCS SELECTION WITH RESPECT TO NBLA

MCS Level	SINR = 5 dB	SINR = 10 dB	SINR = 20 dB
PDF of MCS=0	21.31% higher	40% lower	21.43% lower
PDF of MCS=6	36.84 lower	10.71% higher	4% lower
PDF of MCS=12	10% lower	41.67% higher	16.67% higher

#### G. Analysis of Consumed Resources under Variable Packet Sizes

In SmartCon, since the adaptation is performed based on an intelligent prediction considering the present channel condition, the best possible number of resources are chosen dynamically. From Figs. 8(b) and 9, it is noted that, when the packet size is 500 bytes for an SINR of 20 dB, SmartCon consumes approximately 1.8, 1.11, and 1.32 times less resources than the standard, NANIS, and NBLA mechanisms, respectively. In case of low signal strength (SINR=5dB), the resource consumption in SmartCon are 1.23, 1.12, and 1.16 times lower than the standard, NANIS, and NBLA, respectively.

#### H. Selection of the MCS and Repetitions by SmartCon

Fig. 10 shows the adaptation of the MCS and repetitions in SmartCon, considering the present channel condition. We capture the values of the MCS and repetition numbers selected for the SINR values of the channel. Since we consider several measurements of the aforementioned parameters against the SINR values, we denote such measurements as 'SINR occurrences'. In Fig. 10, the results are shown in three SINR buckets

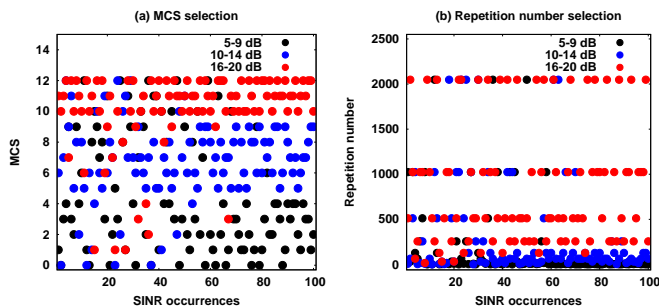


Fig. 10. (a) MCS selection and (b) Repetition number selection

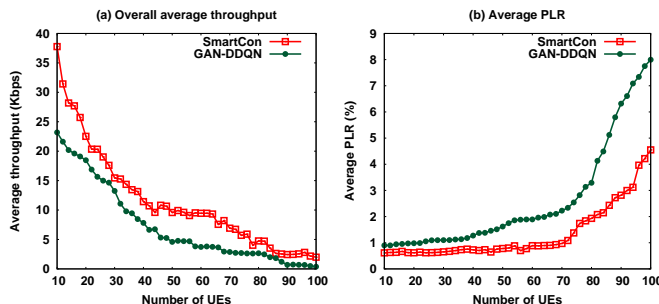


Fig. 11. (a) Average throughput and (b) Average PLR

to demonstrate the impacts of the low, medium, and high signal strength. From Fig. 10(a), it is noted that, higher MCS values are selected for the high SINR values, whereas the MCS level decreases as the signal strength deteriorates. Similarly, to efficiently use the repetition mechanism, the repetition number needs to be increased as the SINR of the channel increases, as illustrated in Fig. 10(b), where it is noted that lower repetition numbers are chosen when the SINR values decrease.

### I. Performance Comparison with GAN-DDQN

Fig. 11 shows the performance improvement of SmartCon over GAN-DDQN considering the average throughput and packet loss rate (PLR). In particular, GAN-DDQN performs dynamic allocation of radio resources considering network slicing in 5G networks. However, SmartCon intelligently selects the MCS values and repetitions, along with the dynamic adaptation of radio resources. Therefore, in SmartCon, the suitable data rate can be set according to the present channel condition, and consequently the average throughput is improved in SmartCon. Fig. 11(a) shows that SmartCon has approximately an average throughput 5.3 times higher than the GAN-DDQN. The GAN-DDQN does not specifically handle the reduction of the packet loss in the network, whereas the proposed GAN is trained with a dataset that is intelligently generated by minimizing the average PLR. As a result, SmartCon provides a significantly lower average PLR than the GAN-DDQN. For instance, when the number of UEs is 50, the average PLR in SmartCon is approximately 52% lower than in GAN-DDQN, as shown in Fig. 11(b).

## VII. CONCLUSION

The proposed GAN models the stochastic time-stamps of traffic scheduling associated with adaptive MCS values, repe-

titions, and number of PRBs. To generate the training dataset for the GAN, we use a MAB-based reinforcement learning mechanism to adapt the MCS, repetitions, and radio resources by considering the present channel condition. The detailed simulation analysis demonstrates that SmartCon significantly boosts the performance of NB-IoT networks. The possible limitation of SmartCon is that periodic re-training is required for adjustments under changing network conditions, which led us to apply an active learning approach. However, SmartCon provides an important step towards the use of deep generative architecture for the optimization of 5G and B5G networks.

The future direction of this work can be an intelligent adaptation of the NPDCCH period length along with dynamic adaptation of the MCS, repetitions, and PRBs. The NPDCCH period is defined as the time interval between two successive NPDCCH, where the eNB should allocate the radio resources for the UEs to receive data. The NPDCCH period significantly affects the utilization of the radio resources in NB-IoT networks, and therefore it is required to smartly handle the NPDCCH period when we dynamically adapt the MCS, repetitions, and PRBs.

## VIII. ACKNOWLEDGEMENT

This work was supported by the Canada Research Chair Program tier-II entitled “Towards a Novel and Intelligent Framework for the Next Generations of IoT Networks”.

## REFERENCES

- [1] A. Bakshi, L. Chen, K. Srinivasan, C. E. Koksal, and A. Eryilmaz, “EMIT: An Efficient MAC Paradigm for the Internet of Things,” in *Proceedings of the 35th Annual IEEE International Conference on Computer Communications (IEEE INFOCOM)*. IEEE, 2016, pp. 1–9.
- [2] S. Popli, R. K. Jha, and S. Jain, “A Survey on Energy Efficient Narrowband Internet of Things (NB-IoT): Architecture, Application and Challenges,” *IEEE Access*, vol. 7, pp. 16 739–16 776, 2019.
- [3] 3GPP RP-161248, 3GPP TSG-RAN Meeting 72, Ericsson, Nokia, ZTE, NTT DOCOMO Inc., Busan, South Korea, “Introduction of NB-IoT in 36.331,” June 2016.
- [4] Y.-P. E. Wang, X. Lin, A. Adhikary, A. Grovlen, Y. Sui, Y. Blankenship, J. Bergman, and H. S. Razaghi, “A Primer on 3GPP Narrowband Internet of Things,” *IEEE Communications Magazine*, vol. 55, no. 3, pp. 117–123, 2017.
- [5] A. Rico-Alvarino, M. Vajapeyam, H. Xu, X. Wang, Y. Blankenship, J. Bergman, T. Tirronen, and E. Yavuz, “An Overview of 3GPP Enhancements on Machine to Machine Communications,” *IEEE Communications Magazine*, vol. 54, no. 6, pp. 14–21, 2016.
- [6] A. D. Zayas and P. Merino, “The 3GPP NB-IoT System Architecture for the Internet of Things,” in *Proceedings of the 2017 IEEE International Conference on Communications Workshops (ICC Workshops)*. IEEE, 2017, pp. 277–282.
- [7] “3rd Generation Partnership Project. Technical Specification 36.211 v13.13.0, Evolved Universal Terrestrial Radio Access (E-UTRA), Physical Channels and Modulation,” <https://www.3gpp.org/DynaReport/36211.htm>, accessed on 02.11.2020.
- [8] S. Ravi, P. Zand, M. El Soussi, and M. Nabi, “Evaluation, Modeling and Optimization of Coverage Enhancement Methods of NB-IoT,” in *Proceedings of the 2019 IEEE 30th Annual International Symposium on Personal, Indoor and Mobile Radio Communications (PIMRC)*. IEEE, 2019, pp. 1–7.
- [9] M. Chafii, F. Bader, and J. Palicot, “Enhancing Coverage in Narrow Band-IoT Using Machine Learning,” in *Proceedings of the 2018 IEEE Wireless Communications and Networking Conference (WCNC)*. IEEE, 2018, pp. 1–6.
- [10] H. Malik, M. M. Alam, H. Pervaiz, Y. Le Moullec, A. Al-Dulaimi, S. Parand, and L. Reggiani, “Radio Resource Management in NB-IoT Systems: Empowered by Interference Prediction and Flexible Duplexing,” *IEEE Network*, vol. 34, no. 1, pp. 144–151, 2019.

- [11] Y.-J. Yu, "NPDCCH Period Adaptation and Downlink Scheduling for NB-IoT Networks," *IEEE Internet of Things Journal*, 2020.
- [12] C. Yu, L. Yu, Y. Wu, Y. He, and Q. Lu, "Uplink Scheduling and Link Adaptation for Narrowband Internet of Things Systems," *IEEE Access*, vol. 5, pp. 1724–1734, 2017.
- [13] J. Wirges and U. Dettmar, "Performance of TCP and UDP over Narrowband Internet of Things (NB-IoT)," in *Proceedings of the 2019 IEEE International Conference on Internet of Things and Intelligence System (IoTais)*. IEEE, 2019, pp. 5–11.
- [14] H. Malik, H. Pervaiz, M. M. Alam, Y. Le Moullec, A. Kuusik, and M. A. Imran, "Radio Resource Management Scheme in NB-IoT Systems," *IEEE Access*, vol. 6, pp. 15 051–15 064, 2018.
- [15] S.-M. Oh and J. Shin, "An Efficient Small Data Transmission Scheme in the 3GPP NB-IoT System," *IEEE Communications Letters*, vol. 21, no. 3, pp. 660–663, 2016.
- [16] X. Chen, Z. Li, Y. Chen, and X. Wang, "Performance Analysis and Uplink Scheduling for QoS-Aware NB-IoT Networks in Mobile Computing," *IEEE Access*, vol. 7, pp. 44 404–44 415, 2019.
- [17] A. E. Mostafa, Y. Zhou, and V. W. Wong, "Connectivity Maximization for Narrowband IoT Systems with NOMA," in *2017 IEEE International Conference on Communications (ICC)*. IEEE, 2017, pp. 1–6.
- [18] B.-Z. Hsieh, Y.-H. Chao, R.-G. Cheng, and N. Nikaiein, "Design of a UE-Specific Uplink Scheduler for Narrowband Internet-of-Things (NB-IoT) Systems," in *Proceedings of the 2018 3rd International Conference on Intelligent Green Building and Smart Grid (IGBSG)*. IEEE, 2018, pp. 1–5.
- [19] R. Ratasuk, N. Mangalvedhe, J. Kaikkonen, and M. Robert, "Data Channel Design and Performance for LTE Narrowband IoT," in *2016 IEEE 84th Vehicular Technology Conference (VTC-Fall)*. IEEE, 2016, pp. 1–5.
- [20] P. R. Manne, S. Ganji, A. Kumar, and K. Kuchi, "Scheduling and Decoding of Downlink Control Channel in 3GPP Narrowband-IoT," *IEEE Access*, vol. 8, pp. 175 612–175 624, 2020.
- [21] Y.-J. Yu and S.-C. Tseng, "Downlink Scheduling for Narrowband Internet of Things (NB-IoT) Systems," in *Proceedings of the 2018 IEEE 87th Vehicular Technology Conference (VTC Spring)*. IEEE, 2018, pp. 1–5.
- [22] C.-W. Huang, S.-C. Tseng, P. Lin, and Y. Kawamoto, "Radio Resource Scheduling for Narrowband Internet of Things Systems: A Performance Study," *IEEE Network*, vol. 33, no. 3, pp. 108–115, 2019.
- [23] O. Elgarhy, L. Reggiani, H. Malik, M. M. Alam, and M. A. Imran, "Rate-Latency Optimization for NB-IoT With Adaptive Resource Unit Configuration in Uplink Transmission," *IEEE Systems Journal*, 2020.
- [24] L. Lei, H. Xu, X. Xiong, K. Zheng, and W. Xiang, "Joint Computation Offloading and Multiuser Scheduling using Approximate Dynamic Programming in NB-IoT Edge Computing System," *IEEE Internet of Things Journal*, vol. 6, no. 3, pp. 5345–5362, 2019.
- [25] A. Azari, Č. Stefanović, P. Popovski, and C. Cavdar, "On the Latency-Energy Performance of NB-IoT Systems in Providing Wide-Area IoT Connectivity," *IEEE Transactions on Green Communications and Networking*, vol. 4, no. 1, pp. 57–68, 2019.
- [26] Y. Hua, R. Li, Z. Zhao, X. Chen, and H. Zhang, "GAN-powered Deep Distributional Reinforcement Learning for Resource Management in Network Slicing," *IEEE Journal on Selected Areas in Communications*, vol. 38, no. 2, pp. 334–349, 2019.
- [27] K. Lei, M. Qin, B. Bai, G. Zhang, and M. Yang, "GCN-GAN: A Non-Linear Temporal Link Prediction Model for Weighted Dynamic Networks," in *Proceedings of the IEEE INFOCOM 2019*. IEEE, 2019, pp. 388–396.
- [28] "NB-IOT - Nsnam," <https://www.nsnam.org/wiki/NB-IOT>, accessed on 02.09.2020.
- [29] J. T. Rolfe, "Discrete Variational Autoencoders," *arXiv preprint arXiv:1609.02200*, 2016.
- [30] M. Shin, D. Jang, H. Nam, K. H. Lee, and D. Lee, "Predicting the Absorption Potential of Chemical Compounds Through a Deep Learning Approach," *IEEE/ACM Transactions on Computational Biology and Bioinformatics*, vol. 15, no. 2, pp. 432–440, 2016.
- [31] Y. Ogata, "On Lewis' Simulation Method for Point Processes," *IEEE Transactions on Information Theory*, vol. 27, no. 1, pp. 23–31, 1981.
- [32] L. Bottou and O. Bousquet, "The Tradeoffs of Large-Scale Learning," *Optimization for Machine Learning*, p. 351, 2011.
- [33] H. Robbins, "Some Aspects of the Sequential Design of Experiments," *Bulletin of the American Mathematical Society*, vol. 58, no. 5, pp. 527 – 535, September 1952.
- [34] C. Watkins, "Learning from Delayed Rewards. PhD thesis, University of Cambridge, Cambridge, England," May 1989.
- [35] P. Auer, N. Cesa-Bianchi, and P. Fischer, "Finite-time Analysis of the Multiarmed Bandit Problem," *Journal Machine Learning*, vol. 47, no. 2, pp. 235–256, May 2002.
- [36] A. Saha, N. Ganguly, S. Chakraborty, and A. De, "Learning network traffic dynamics using temporal point process," in *Proceedings of the 2019 IEEE INFOCOM*. IEEE, 2019, pp. 1927–1935.